S. G. Mao
A. Y. T. Leung
Department of Civil and Structural
Engineering
University of Hong Kong
Hong Kong

Symplectic Integration and Nonlinear Dynamic Symmetry Breaking of Frames

An accurate beam finite element is used to solve nonlinear vibration of arched beams and framed structures. The nonlinear governing equations of a skeletal structure are integrated numerically using symplectic integration schemes so that the Poincaré integral invariant of a Hamiltonian flow are preserved during the evolution. The element stiffness matrices are not required to be assembled into global form, because the integration is completed on an element level so that many elements can be handled in core by a small computer. Testing examples include arched beams and frames with and without damping in free and forced vibration. The dynamic symmetry breaking phenomena are noted at the dynamic buckling point. © 1995 John Wiley & Sons, Inc.

INTRODUCTION

The geometric nonlinear analyses of framed structure for both static and dynamic loading are of considerable interest and practical importance. Chajes and Churchill (1987) and Meek and Tan (1984) considered the influence of higher order nonlinear terms and gave the stiffness matrix expressions accurately. But considerable efforts have been concentrated on the tangent or secant stiffness matrices that consider geometric nonlinearity of various degrees. In our previous paper (Leung and Mao, 1995), the second- and third-order nonlinear stiffness matrices were introduced by the order of nodal displacements. The equilibrium equations were accurately discretized and an explicit beam finite element was established. The dynamic problems of beams with large displacement and small strain and ro-

tation have been solved. Using the explicit beam finite element, both programming and computing the strain energy of the discretized systems and the derivatives of the strain energy with respect to the nodal displacements are convenient and are more advantageous.

In this article, a previously developed beam finite elements formulation (Leung and Mao, 1995) is extended to framed structures. The symplectic numerical integration schemes (Feng and Qin, 1991; Ruth, 1983; Wu, 1988) are applied to solve the equations element by element without forming the global matrices. This makes it possible to solve nonlinear vibrations of large framed structures using a small computer. Symplectic integration schemes are used. Emphasis is on the asymmetric response of symmetric structures subject to symmetric dynamic loads.

LAGRANGIAN EQUATIONS

For an initially straight Euler–Bernoulli beam undergoing large displacement with small strain and small rotation, the axial strain ε_x at the centroid of the cross section can be expressed as (Crisfield, 1991)

$$\varepsilon_x = \frac{\partial u}{\partial x} + \frac{1}{2}\left(\frac{\partial w}{\partial x}\right)^2. \tag{1}$$

Assuming plane sections remain plane, the displacement in the x direction u^z and the strain ε_x^z at distance z from the centroid are given by

$$u^z = u - z\frac{dw}{dx}, \quad \varepsilon_x^z = \varepsilon_x + z\chi,$$

where the curvature χ is defined as

$$\chi = -\frac{\partial^2 w}{\partial x^2}.$$

Here $u(x, t)$ and $w(x, t)$ are the axial and transverse displacements of the neutral axis, respectively. The axial resultant force S and the bending moment M are related to ε_x and χ and are

$$S = EA\varepsilon_x, \quad M = EI\chi,$$

where E is Young's modulus, A the cross sectional area, and I the second moment of area of the cross section. The corresponding Lagrangian for an undamped beam of length l is

$$L = \frac{1}{2}\int_0^l \rho A\left[\left(\frac{\partial u}{\partial t}\right)^2 + \left(\frac{\partial w}{\partial t}\right)^2\right] dx$$

$$- \frac{1}{2}\int_0^l (EA\varepsilon_x^2 + EI\chi^2)\, dx \tag{3}$$

$$+ \int_0^l (F_u u + F_w w)\, dx$$

where ρ is the mass density of material, t is the time variable, and $F_u(x, t)$ and $F_w(x, t)$ are the axial and transverse loads, respectively.

FINITE ELEMENT DISCRETIZATION

Consider an initially straight beam, the displacements $u(x, t)$ and $w(x, t)$ are interpolated by their nodal values $\mathbf{u}(t)$, $\mathbf{w}(t)$, respectively, so that

$$u(x, t) = [\mathbf{n}(x)]\{\mathbf{u}(t)\},$$
$$w(x, t) = [\mathbf{N}(x)]\{\mathbf{w}(t)\}. \tag{4}$$

where $[\mathbf{N}(x)] = [1 - 3\xi^2 + 2\xi^3,\ \xi(\xi^2 - 2\xi + 1)l,\ 3\xi^2 - 2\xi^3,\ (\xi^3 - \xi^2)l]$, and $[\mathbf{n}(x)] = [1 - \xi,\ \xi]$ are the shape functions and $\xi = x/l$. After integration, Eq. (3) will be discretized into

$$\begin{aligned}
L = &\ \frac{1}{2}\{\dot{\mathbf{u}}\}^T[\mathbf{M}_u]\{\dot{\mathbf{u}}\} + \frac{1}{2}\{\dot{\mathbf{w}}\}^T[\mathbf{M}_w]\{\dot{\mathbf{w}}\} \\
&- \frac{1}{2}\{\mathbf{u}\}^T[\mathbf{K}_u]\{\mathbf{u}\} - \frac{1}{2}\{\mathbf{w}\}^T[\mathbf{K}_w]\{\mathbf{w}\} \\
&- \frac{1}{2}\{\mathbf{u}\}^T[\mathbf{K}_{uq}]\{\mathbf{w}_q\} - \frac{1}{8}\{\mathbf{w}_q\}^T[\mathbf{K}_q]\{\mathbf{w}_q\} \\
&+ \{\mathbf{F}_u\}^T\{\mathbf{u}\} + \{\mathbf{F}_w\}^T\{\mathbf{w}\},
\end{aligned} \tag{5}$$

where, for the element e with node i and node j,

$$\{\mathbf{w}^e\} = \{w_i, \theta_i, w_j, \theta_j\}, \quad \{\mathbf{u}^e\} = \{u_i, u_j\}.$$

$$[\mathbf{M}_u^e] = \int_0^l \rho A[\mathbf{n}]^T[\mathbf{n}]\, dx, \quad [\mathbf{M}_w^e] = \int_0^l \rho A[\mathbf{N}]^T[\mathbf{N}]\, dx.$$

$$[\mathbf{K}_u^e] = \int_0^l EA[\mathbf{n}_{,x}]^T[\mathbf{n}_{,x}]\, dx,$$

$$[\mathbf{K}_w^e] = \int_0^l EI[\mathbf{N}_{,xx}]^T[\mathbf{N}_{,xx}]\, dx,$$

$$\{\mathbf{F}_u^e\} = \int_0^l [\mathbf{n}]^T F_u\, dx, \quad \{\mathbf{F}_w^e\} = \int_0^l [\mathbf{N}]^T F_w\, dx.$$

The following terms are new: the quadratic nodal displacement

$$\begin{aligned}
\{\mathbf{w}_q^e\} = \{&w_i^2,\ w_i\theta_i,\ w_iw_j, \\
&w_i\theta_j,\ \theta_i^2,\ \theta_iw_j,\ \theta_i\theta_j,\ w_j^2,\ w_j\theta_j,\ \theta_j^2\};
\end{aligned}$$

the second-order stiffness matrix

$$[\mathbf{K}_{uq}^e] = \int_0^l EA[\mathbf{n}_{,x}]^T[\mathbf{Q}]\, dx;$$

and the third-order stiffness matrix

$$[\mathbf{K}_q^e] = \int_0^l EA[\mathbf{Q}]^T[\mathbf{Q}]\, dx,$$

in which $[\mathbf{Q}]$ is defined by the interpolation, $(\partial w/\partial x)^2 = [\mathbf{Q}]\{\mathbf{w}_q^e\}$ and is given by

$$[\mathbf{Q}] = \left[\frac{36}{l^2} (\xi^2 - 2\xi^3 + \xi^4), \quad \frac{12}{l} (-\xi + 5\xi^2 - 7\xi^3 + 3\xi^4), \quad \frac{72}{l^2} (-\xi^2 + 2\xi^3 - \xi^4), \right.$$

$$\frac{12}{l} (2\xi^2 - 5\xi^3 + 3\xi^4), \quad 1 - 8\xi + 22\xi^2 - 24\xi^3 + 9\xi^4, \quad \frac{12}{l} (\xi - 5\xi^2 + 7\xi^3 - 3\xi^4),$$

$$2(-2\xi + 11\xi^2 - 18\xi^3 + 9\xi^4), \quad \frac{36}{l^2} (\xi^2 - 2\xi^3 + \xi^4), \quad \frac{12}{l} (-2\xi^2 + 5\xi^3 - 3\xi^4),$$

$$\left. 4\xi^2 - 12\xi^3 + 9\xi^4 \right].$$

An overdot denotes differentiation with respect to t. The matrices $[\mathbf{K}_{uq}^e]$ and $[\mathbf{K}_q^e]$, which are independent of the nodal displacements, are given explicitly in Leung and Mao (1995). The others are available in most of the references.

SYMPLECTIC INTEGRATION SCHEMES

The Lagrangian formulation is more popular than the Hamiltonian because the former uses physical quantities directly in the configuration space. The Hamiltonian methods are not particularly superior to Lagrangian techniques for the direct solution of mechanical problems. Rather, the usefulness of the Hamiltonian viewpoint lies in the invariant symplectic structure of the resulting equations that will be very convenient in theoretical and numerical studies.

All dynamic evolutions of Hamiltonian systems are symplectic (canonical) transformation; the time discretization algorithm should also be symplectic. Ruth (1983), Feng and Qin (1991), and Feng et al. (1989) developed some symplectic integration methods for Hamiltonian systems. Simo et al. (1992) gave second-order accurate methods, which preserved both momentum and energy exactly, and a detailed discussion to exact energy–momentum conserving algorithms and symplectic schemes for nonlinear dynamics. Robert and Pau (1992) discussed the accuracy of symplectic integrators in the energy error. Wu (1988) proposed the time-centered Euler scheme with second-order accuracy to an arbitrary mth-order accuracy for ordinary different equations.

Assuming that the mechanical systems are holonomic and that the forces are monogenic, then the dynamic evolution problems may be expressed in the canonical system of differential equations:

$$\frac{\partial \mathbf{p}}{\partial t} = -H_q(\mathbf{p}, \mathbf{q}, t),$$

$$\frac{\partial \mathbf{q}}{\partial t} = H_p(\mathbf{p}, \mathbf{q}, t). \tag{6}$$

for a given Hamiltonian H. The Hamiltonian is reduced to the energy function $H(p_1, \ldots, p_n, q_1, \ldots, q_n, t)$ for the inertial frame of reference, where $H_p = \partial H/\partial \mathbf{p}$, $H_q = \partial H/\partial \mathbf{q}$.

Before discussing nonautonomous systems, let us consider the autonomous Hamiltonian system when H is independent on time,

$$\dot{\mathbf{z}} = \mathbf{J} \frac{\partial H}{\partial \mathbf{z}}, \quad \mathbf{z} \in \mathbf{R}^{2n}, \tag{7}$$

where

$$\mathbf{J} = \begin{bmatrix} \mathbf{0} & -\mathbf{1} \\ \mathbf{1} & \mathbf{0} \end{bmatrix}.$$

Here **1** is the standard $n \times n$ unit matrix and **0** is the $n \times n$ zero matrix, and $z_i = p_i$, $z_{i+n} = q_i$; $i \leq n$, n is the number of degrees of freedom. Its phase flow is denoted as $g^t(\mathbf{z}) = g(\mathbf{z}, t) = g_H(\mathbf{z}, t)$, being a one-parameter group of canonical maps (Abraham and Mardsen, 1978; Arnold, 1978) i.e.,

$$g^0 = \text{identity}, \quad g^{t_1 + t_2} = g^{t_1} g^{t_2}$$

and if $\mathbf{z}_0$ is taken as an initial condition, then $\mathbf{z}(t) = g^t(\mathbf{z}_0)$ is the solution of (7) with the initial values $\mathbf{z}_0$. Different symplectic integration schemes for the system (7) have been constructed (Feng and Qin, 1991). Symplectic schemes for Hamiltonian systems preserve all the linear conservative quantities. Moreover, the implicit time-centered symplectic scheme preserves all the linear and quadratic conservative quantities. Let us consider the first-order and the second-order canonical difference schemes for Eq. (7),

$$p_i^{k+1} = p_i^k - hH_{q_i}(\mathbf{p}^{k+1}, \mathbf{q}^k),$$

$$q_i^{k+1} = q_i^k + hH_p(\mathbf{p}^{k+1}, \mathbf{q}^k). \tag{8}$$

$$p_i^{k+1} = p_i^k - hH_{q_i}(\mathbf{p}^{k+1}, \mathbf{q}^k)$$

$$-\frac{h^2}{2}\left(\sum_{j=1}^{n} H_{q_j}H_{p_j}\right)_{q_i}(\mathbf{p}^{k+1}, \mathbf{q}^k),$$

$$q_i^{k+1} = q_i^k + hH_{p_i}(\mathbf{p}^{k+1}, \mathbf{q}^k) \qquad (9)$$

$$+\frac{h^2}{2}\left(\sum_{j=1}^{n} H_{q_j}H_{p_j}\right)_{p_i}(\mathbf{p}^{k+1}, \mathbf{q}^k),$$

where h is the time step. These schemes are explicit with respect to the coordinate **q** and are *A* stable. In general, the Hamiltonian for nonlinear vibration problems of structures is separable, i.e., $H = U(\mathbf{p}) + V(\mathbf{q})$, where $U(\mathbf{p})$ is quadratic in **p** representing the kinetic energy. Thus, in this case, Eqs. (8) and (9) are a set of linear equations in **p**. The time-centered Euler scheme (Feng and Qin, 1991) for Eq. (7) is

$$\mathbf{z}^{k+1} = \mathbf{z}^k + hJH_z\left(\frac{\mathbf{z}^{k-1} + \mathbf{z}^k}{2}\right), \qquad (10)$$

which may be written further in

$$p_i^{k+1} = p_i^k - hH_{q_i}\left(\frac{\mathbf{p}^{k+1} + \mathbf{p}^k}{2}, \frac{\mathbf{q}^{k+1} + \mathbf{q}^k}{2}\right), \qquad (10a)$$

$$q_i^{k+1} = q_i^k + hH_p\left(\frac{\mathbf{p}^{k+1} + \mathbf{p}^k}{2}, \frac{\mathbf{q}^{k+1} + \mathbf{q}^k}{2}\right). \qquad (10b)$$

The scheme (10) is an implicit second-order scheme. Thus scheme (10) requires iterations while schemes (8) and (9) do not.

For nonautonomous Hamiltonian systems, we regard the time t as an additional dependent variable. That is, letting $q_{n+1} = t$, we can choose a parameter τ as a new independent variable. It is well known (Goldstein, 1980) that

$$p_{n+1} = -H,$$

which has a unit of energy, is the generalized momentum conjugate to the time t. For this special choice, the function $K(\mathbf{w}) = p_{n+1} + H(\mathbf{z})$ with $\mathbf{w} = (q_1, \ldots, q_n, t, p_1, \ldots, p_n, -H)^T$ will take the place of the Hamiltonian function H.

Consider the ordinary differential equation (ODE),

$$\frac{d\mathbf{x}}{dt} = \mathbf{F}(\mathbf{x}) \qquad (11)$$

where $\mathbf{F}: \mathbf{R}^N \rightarrow \mathbf{R}^N$ is an analytic function in $\mathbf{R}^N$,

$$\mathbf{F} = (F_1, F_2, \ldots, F_N)^T.$$

For time-dependent ODEs, we use a new time variable τ to make the system time independent. Let $t = \tau$ and

$$\frac{dt}{d\tau} = 1,$$

then the time-dependent ODEs in $\mathbf{R}^N$ can be rewritten as time-independent equations in $\mathbf{R}^{N+1}$.

To make a set of ODEs into a Hamiltonian system, we introduce a matching system (Wu, 1988)

$$\frac{d\mathbf{X}}{dt} = -(\mathbf{X}^T\mathbf{F}'(\mathbf{x}))^T,$$

$$\mathbf{F}'(\mathbf{x}) = \frac{D\mathbf{F}}{D\mathbf{x}}. \qquad (12)$$

Assuming that the Hamiltonian $H = \mathbf{X}^T\mathbf{F}(\mathbf{x})$, the systems (11) and (12) together can be rewritten as a Hamiltonian system

$$\frac{d\mathbf{x}}{dt} = \frac{\partial H}{\partial \mathbf{X}},$$

$$\frac{d\mathbf{X}}{dt} = -\frac{\partial H}{\partial \mathbf{x}}. \qquad (13)$$

Wu (1988) gave a time-centered Euler scheme with second-order accuracy to an arbitrary mth-order accuracy for system (13). This scheme is L stable. The second time-centered Euler scheme is

$$x_i^{k+1} = x_i^k + hF_i\left(\frac{\mathbf{x}^k + \mathbf{x}^{k+1}}{2}\right). \qquad (14)$$

This is an implicit second-order scheme independent of the matching system (12).

If the Hamiltonian system (6) is separable, then

$$H = U(\mathbf{p}) + V(\mathbf{q}, t). \qquad (15)$$

Ruth (1983) constructed a third-order explicit symplectic scheme for the separable Hamiltonian (15). Qin et al. (1991) constructed a fourth-order explicit symplectic difference scheme.

We may use the different symplectic integration schemes mentioned above to solve Hamiltonian equations. From the viewpoint of computational stability, implicit schemes are better. For explicit schemes, variable time steps may be used to guarantee the stability of computation. The time step is controlled by the superior and

inferior limits of motion, i.e., $|q_i^{k+1} - q_i^k| \le \varepsilon$ or $|x_i^{k+1} - x_i^k| \le \varepsilon$. In this work we use the first-order scheme (8) and the time-centered Euler schemes (10) and (14) for the numerical examples below.

FINITE ELEMENT EQUATIONS OF MOTION

For an initially straight beam, the finite element equations are obtained from Eq. (3) by the Hamilton principle,

$$[\mathbf{M}_u]\{\ddot{\mathbf{u}}\} + [\mathbf{K}_u]\{\mathbf{u}\} + \tfrac{1}{2}[\mathbf{K}_{uq}]\{\mathbf{w}_q\} = \{\mathbf{F}_u\},$$

$$[\mathbf{M}_w]\{\ddot{\mathbf{w}}\} + [\mathbf{K}_w]\{\mathbf{w}\}$$

$$+ \tfrac{1}{2}[\mathbf{w}_{q,w}]^T[\mathbf{K}_{uq}]^T\{\mathbf{u}\} + \tfrac{1}{4}[\mathbf{w}_{q,w}]^T[\mathbf{K}_q]\{\mathbf{w}_q\} = \{\mathbf{F}_w\}, \qquad (16)$$

where the subscript $(,w)$ denotes differentiation with respect to $\{\mathbf{w}\}$. For damped forced vibration problems, the finite element equations are obtained by adding the appropriated damping terms,

$$[\mathbf{M}_u]\{\ddot{\mathbf{u}}\} + [\mathbf{C}_u]\{\dot{\mathbf{u}}\} + [\mathbf{K}_u]\{\mathbf{u}\} + \tfrac{1}{2}[\mathbf{K}_{uq}]\{\mathbf{w}_q\} = \{\mathbf{F}_u\},$$

$$[\mathbf{M}_w]\{\ddot{\mathbf{w}}\} + [\mathbf{C}_w]\{\dot{\mathbf{w}}\} + [\mathbf{K}_w]\{\mathbf{w}\}$$

$$+ \tfrac{1}{2}[\mathbf{w}_{q,w}]^T[\mathbf{K}_{uq}]^T\{\mathbf{u}\} + \tfrac{1}{4}[\mathbf{w}_{q,w}]^T[\mathbf{K}_q]\{\mathbf{w}_q\} = \{\mathbf{F}_w\}, \qquad (17)$$

where $[\mathbf{C}_u]$, $[\mathbf{C}_w]$ are the corresponding damping matrices.

Equations (16) and (17) are different from some existing references, such as Yang and Saigal (1984) in that the induced axial force S is a function of displacements and is not averaged and, in finite element discretization, Eq. (3) has not been linearized, i.e., the discretization is more accurate. Due to the accurate discretization, iteration procedures are not needed in calculating every incremental step. The accuracy for the unaveraged S is important in the study of nonlinear vibrations, chaos, and bifurcations.

Now, we use the Hamiltonian formalism. For free vibration and undamped forced vibration problems the Hamiltonian of the Lagrangian (3) is obtained by the method introduced in Goldstein (1980),

$$H = \tfrac{1}{2}\{\mathbf{p}_u\}^T[\mathbf{M}_u]^{-1}\{\mathbf{p}_u\} + \tfrac{1}{2}\{\mathbf{p}_w\}^T[M_w]^{-1}\{\mathbf{p}_w\}$$

$$+ \tfrac{1}{2}\{\mathbf{u}\}^T[\mathbf{K}_u]\{\mathbf{u}\}$$

$$+ \tfrac{1}{2}\{\mathbf{w}\}^T[\mathbf{K}_w]\{w\} + \tfrac{1}{2}\{\mathbf{u}\}^T[\mathbf{K}_{uq}]\{\mathbf{w}_q\} \qquad (18)$$

$$+ \tfrac{1}{8}\{\mathbf{w}_q\}^T[\mathbf{K}_q]\{\mathbf{w}_q\}$$

$$- \{\mathbf{F}_u\}^T\{\mathbf{u}\} - \{\mathbf{F}_w\}^T\{\mathbf{w}\},$$

where $\{\mathbf{p}_u\} = [\mathbf{M}_u]\{\dot{\mathbf{u}}\}$, $\{\mathbf{p}_w\} = [\mathbf{M}_w]\{\dot{\mathbf{w}}\}$ are the momenta. Hamilton's equations corresponding to Eq. (18) are

$$\frac{\partial\{\mathbf{u}\}}{\partial t} = [\mathbf{M}_u]^{-1}\{\mathbf{p}_u\},$$

$$\frac{\partial\{\mathbf{w}\}}{\partial t} = [\mathbf{M}_w]^{-1}\{\mathbf{p}_w\},$$

$$\frac{\partial\{\mathbf{p}_u\}}{\partial t} = -[\mathbf{K}_u]\{\mathbf{u}\} - \tfrac{1}{2}[\mathbf{K}_{uq}]\{\mathbf{w}_q\} + \{\mathbf{F}_u\}, \qquad (19)$$

$$\frac{\partial\{\mathbf{p}_w\}}{\partial t} = -[\mathbf{K}_w]\{\mathbf{w}\} - \tfrac{1}{2}[\mathbf{w}_{q,w}]^T[\mathbf{K}_{uq}]^T\{\mathbf{u}\}$$

$$- \tfrac{1}{4}[\mathbf{w}_{q,w}]^T[\mathbf{K}_q]\{\mathbf{w}_q\} + \{\mathbf{F}_w\}.$$

For damped forced vibration problems, extended Hamiltonian equations are obtained by writing Eq. (17) in the form of Eq. (11)

$$\{\dot{\mathbf{U}}\} = -[\mathbf{M}_u]^{-1}([\mathbf{C}_u]\{\mathbf{U}\} + [\mathbf{K}_u]\{\mathbf{u}\}$$

$$+ \tfrac{1}{2}[\mathbf{K}_{uq}]\{\mathbf{w}_q\} - \{\mathbf{F}_u\}),$$

$$\{\dot{\mathbf{W}}\} = -[\mathbf{M}_w]^{-1}([\mathbf{C}_w]\{\mathbf{W}\} + [\mathbf{K}_w]\{\mathbf{w}\} \qquad (20)$$

$$+ \tfrac{1}{2}[\mathbf{w}_{q,w}]^T[\mathbf{K}_{uq}]^T\{\mathbf{u}\}$$

$$+ \tfrac{1}{4}[\mathbf{w}_{q,w}]^T[\mathbf{K}_q]\{\mathbf{w}_q\} - \{\mathbf{F}_w\}),$$

$$\{\dot{\mathbf{u}}\} = \{U\}, \quad \{\dot{\mathbf{w}}\} = \{W\}.$$

For an initially straight beam, forming general stiffness matrices $[\mathbf{K}_{uq}]$ and $[\mathbf{K}_q]$ is not complicated (Leung and Mao, 1995). But for framed structures with many elements, computing the general nonlinear stiffness matrices is of some complexity. However, when one uses explicit integration schemes, the global stiffness matrices are not needed. Thus we may integrate the Hamiltonian equations element by element.

For an arbitrarily oriented beam element in the plane, the nodal displacements of the ith node in terms of local coordinates of element e, $\{\mathbf{d}_i^e\}$, and those in terms of global coordinates $\{\mathbf{d}_i\}$ are related by

$$\begin{Bmatrix} u_i^e \\ v_i^e \\ \theta_i^e \end{Bmatrix} = \begin{bmatrix} \lambda & \mu & 0 \\ -\mu & \lambda & 0 \\ 0 & 0 & 1 \end{bmatrix} \begin{Bmatrix} u_i \\ v_i \\ \theta_i \end{Bmatrix} \qquad (21a)$$

or symbolically

$$\{\mathbf{d}_i^e\} = [\mathbf{T}_1]\{\mathbf{d}_i\} \qquad (21b)$$

where $\lambda = \cos \alpha$ and $\mu = \sin \alpha$ with α being the angle of orientation of the beam. The Hamiltonian may be written on the element level,

$$H = \tfrac{1}{2} \{\mathbf{p}_d\}^T [\mathbf{M}_d]^{-1} \{\mathbf{p}_d\} + \sum_e (\tfrac{1}{2} \{\mathbf{u}^e\}^T [K_{tt}^e] \{\mathbf{u}^e\}$$

$$+ \tfrac{1}{2} \{\mathbf{w}^e\}^T [\mathbf{K}_w^e] \{\mathbf{w}^e\}$$

$$+ \tfrac{1}{2} \{\mathbf{u}^e\}^T [\mathbf{K}_{uq}^e] \{\mathbf{w}_q^e\} + \tfrac{1}{8} \{\mathbf{w}_q^e\}^T [\mathbf{K}_q^e] \{\mathbf{w}_q^e\} \qquad (22a)$$

$$- \{\mathbf{F}_u^e\}^T \{\mathbf{u}^e\} - \{\mathbf{F}_w^e\}^T \{\mathbf{w}^e\}),$$

where $[\mathbf{M}_d]$ is the conventional global mass matrix in terms of global coordinates and $\{\mathbf{p}_d\} = [\mathbf{M}_d] \{\dot{\mathbf{d}}\}$ are the momenta. Denote the expression after $\sum_e$ in Eq. (22a) by V_1^e, then Eq. (22a) may be written as

$$H = \frac{1}{2} \{\mathbf{p}\}^T [\mathbf{M}_d]^{-1} \{\mathbf{p}\} + \sum_e V_1^e. \qquad (22b)$$

$V_1^e = U_1^e + \Omega_1^e$ is the total potential energy of element e, with U_1^e being the strain energy and Ω_1^e the potential energy of external forces. The first- and the second-order derivatives of V_1^e with respect to $\{\mathbf{d}\}$ are easily computed. Thus, the Hamiltonian equations corresponding to Eq. (22a) may be obtained. For damped forced vibration problems, the finite element equations are obtained by adding the appropriate damping terms,

$$[\mathbf{M}_d]\{\ddot{\mathbf{d}}\} + [\mathbf{C}_d]\{\dot{\mathbf{d}}\} + \left(\sum_e V_1^e \right)_{,d} = 0 \qquad (23)$$

where $[\mathbf{C}_d]$ are the corresponding damping matrices. Equation (23) may be rewritten in the form of Eq. (20).

NUMERICAL EXAMPLES

In the case of transient excitation by pulses (i.e., shock load, explosions, etc.), damping has very little effect on the response qualitatively, so an undamped analysis is generally adequate. However in the case of steady-state vibration, damping is relatively important. Several examples on the dynamics of nonlinear structures with and without damping are presented. The material of the structures is isotopic linear elastic. Results are compared with those of other investigators when possible. Example 1 and example 2 were

calculated previously in Leung and Mao (1995) by means of forming all global stiffness matrices that gave the same results as in this study working on the element matrices only.

Example 1: Undamped Forced Vibration of a Clamped–Clamped Beam by Sudden Load

A clamped–clamped beam under a static concentrated force of 2843.919 N acting at the midspan at time $t = 0$ is considered. The modulus of elasticity is $E = 2.07 \times 10^8$ kN/m², the mass density is $\rho = 2.71 \times 10^{-3}$ kg/cm³, the length is $l = 50.8$ cm, and the cross section is 2.54×0.3175 cm. The beam geometry with a concentrated load is shown in Fig. 1. Because of symmetry, one-half of the beam is modeled by six finite elements. Figure 2 gives the nonlinear responses of the midspan deflection obtained using the time-centered Euler scheme with an equal time step, $\Delta t = 1$ μs. Figures 3 and 4 give the total energy $E =$ kinetic energy $K +$ potential energy V and the total kinetic energy K, respectively.

This problem has been studied by many investigators. Mondkar and Powell (1977) used five 8-node plane stress elements to model one-half of the beam. Yang and Saigal (1984) used six beam elements with $\Delta t = 5$ μs and $\Delta t = 10$ μs. McNamara (1974) used five beam bending elements based on a central-difference operator with $\Delta t = 5$ μs. The maximum displacement and the period of the first cycle were 0.02286 m and 2884 μs in McNamara (1974), 0.019558 m and 2300 μs in Mondkar and Powell (1977) and Yang and Saigal (1984), and 0.019456 m and 2151 μs in this study.

Simo et al. (1992) and Crisfield and Shi (1994) explored that the time-centered Euler scheme is the idea of a "midpoint equilibrium." For nonlin-
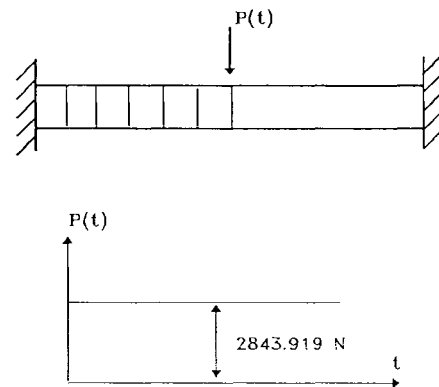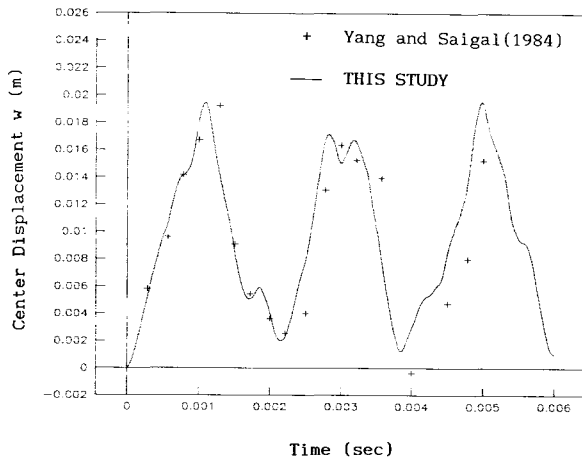

FIGURE 1   Beam under concentrated load.

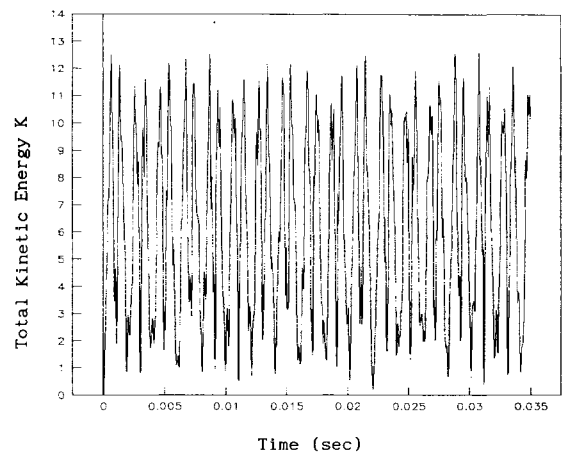**FIGURE 2** Midspan displacement of a clamped beam.
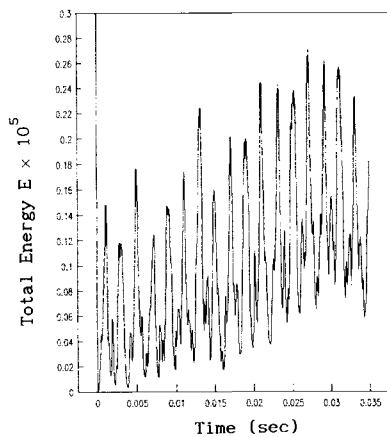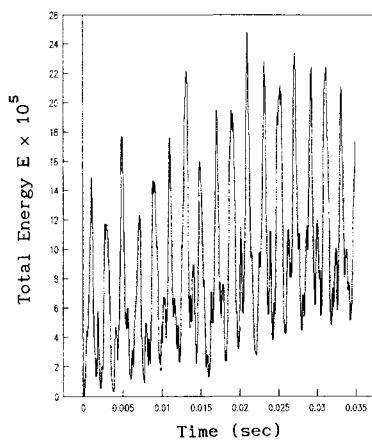

FIGURE 4 Total kinetic energy K, $\Delta t = 1$ μs.

(a) $\Delta t = 0.1$ μsec

(b) $\Delta t = 1$ μsec

FIGURE 3 Total energy E.

ear Hamiltonian systems the time-centered Euler scheme fails to conserve the total energy of the system (Simo et al., (1992). But from Figs. 3 and 4 we may know that the amplitude is very small referring to the total kinetic energy, and the total energy is almost preserved when using small time steps.

Example 2: Damped Forced Vibrations of a Hinged–Hinged Beam by Harmonic Force

Consider a hinged–hinged uniform beam with immovable edges under a concentrated force of F cos ωt acting at the midspan, where $F = 2.0 \times 10^{-3}$, $\omega = 1.1$ ω_L, where ω_L is the linear natural frequency $\omega_L = 3.4189 \times 10^{-3}$. The modulus of elasticity, $E = 1$; the mass density, $\rho = 1$; the length, $l = 28.8675$; the second moment of inertia, $I = 0.083333$; and the cross-sectional area, $A = 1.0$. Assume the damping forces are proportional to the mass matrix, i.e., $C = \alpha M$, and damping ratio $\alpha = 0.01$. Because of symmetry, one-half of the beam was modeled by four finite elements. We use the time-centered Euler scheme with a variable time step. The response curve is shown in Fig. 5. The phase plane trajectories of steady-state motion are shown in Fig. 6.

Example 3: Elastic Dynamic Snap Buckling of an Arch

A dynamic buckling analysis of the circular arch shown in Fig. 7 was carried out. Due to symmetry, one-half of the arch is modeled by nine finite elements. Figure 8 shows the displacement response predicted in this study using the time-
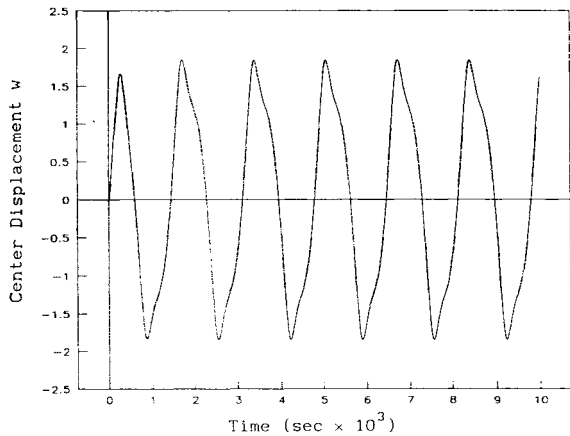
FIGURE 5   Midspan displacement of a hinged beam.
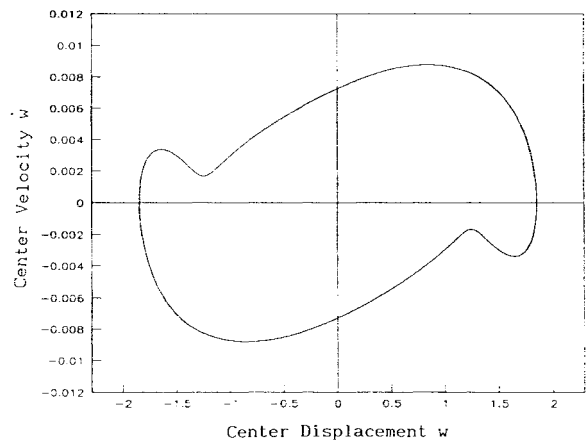

FIGURE 6   Midspan phase plane trajectories of steady-state motion of a hinged beam.

centered Euler scheme. In Fig. 8, the deflection δ defined as

$$\delta = \frac{\text{vertical displacement at apex}}{\text{average rise to arch} = H/2}$$

is used. The dynamic buckling of the arch occurs at the load level at which a sudden increase in the

deflection ratio is measured. Figure 8 shows that at $P_0 = 0.202$, it oscillates about a position of approximately $\delta = -0.5$, and that at $P_0 = 0.203$ it snaps through at $\tau = 60.0$, and it oscillates about a position of approximately $\delta = -4.0$. Therefore, for τ from 0 to 90.0, the buckling load predicted here lies between $\Pi_0 = 0.202$ and $P_0 = 0.203$. For
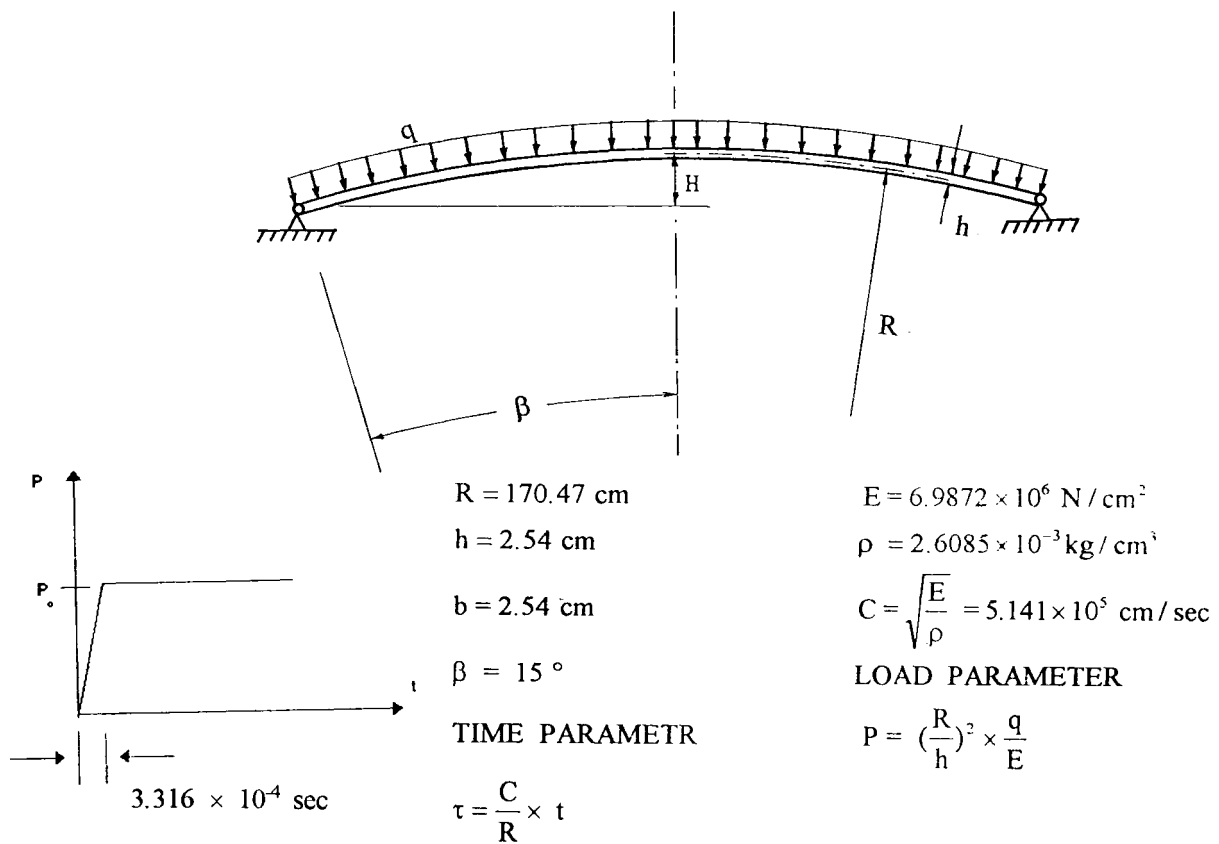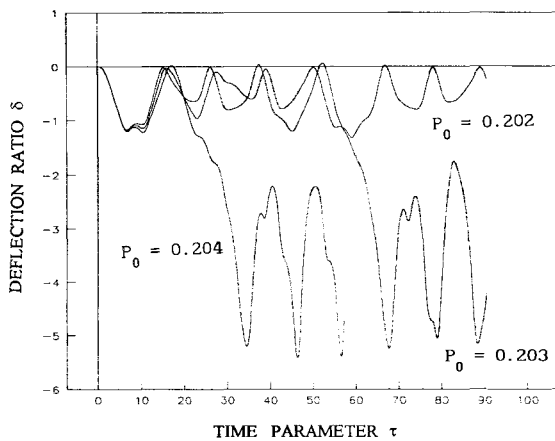

$R = 170.47$ cm

$h = 2.54$ cm

$b = 2.54$ cm

$\beta = 15°$

TIME PARAMETR

$$\tau = \frac{C}{R} \times t$$

$E = 6.9872 \times 10^6$ N / cm^2

$\rho = 2.6085 \times 10^{-3}$ kg / cm^3

$C = \sqrt{\frac{E}{\rho}} = 5.141 \times 10^5$ cm / sec

LOAD PARAMETER

$$P = (\frac{R}{h})^2 \times \frac{q}{E}$$

3.316×10^{-4} sec

**FIGURE 7**   Simply supported shallow arch.

FIGURE 8 Dynamic snap-through of a shallow circular arch.

τ from 0 to 50, the buckling load predicted here lies between $P_0 = 0.203$ and $P_0 = 0.204$, which is about 2.0% higher than that predicted by Bathe et al. (1975). Moreover, results obtained using the whole arch are the same as those using one-half of the arch.

Example 4: Dynamic Analysis of Plane Frames

The geometry for the frame is given in Fig. 9, where the modulus of elasticity is $E = 2.07 \times 10^8$ kN/m^2, the mass density is $\rho = 2.71 \times 10^{-3}$ kg/cm^3, and the cross section is 25.4×3.175 cm. Every beam member is modeled by four elements.

For the undamped case, nonlinear responses to different concentrated load $P(t) = F_c$ acting at the top point of the frame are shown in Fig. 10(a–e) and Figure 11. In Fig. 10(e) we give the linear solution obtained using the whole frame for $F_c = 120$ kN. The nonlinear subharmonic solutions are obvious. Intuitively, due to symmetry, results obtained using one-half of the frame should be
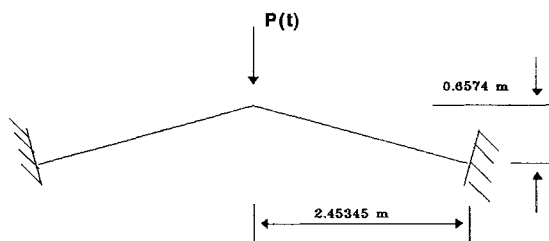

FIGURE 9 Plane frame under concentrated load.

the same as using the whole frame. However, in numerical calculations, the difference is very large in some cases, when antisymmetric modes are resonated by the nonlinear frequency. In such cases, the symmetric solutions obtained using one-half the frame are, in fact, unstable. The lower branches of Figs. 10 and 11 show the symmetry breaking branches. Moreover, Fig. 10 (a–e) show a comparison of the nonlinear responses for different loads. With F_c increasing, the symmetry breaking emerges more easily. Here, we have not introduced any small perturbations artificially to obtain the asymmetric deformation, which is different from the usual references. For example, Wood and Zienkiewicz (1977) calculated the asymmetric deformation of a two-hinged deep arch by imposing a small perturbation to the radius of the arch. Of course, the rounding error of computers may be regarded as small perturbations. Figures 10(a–e) also show a comparison of the linear and nonlinear response. The considerable difference in the maximum displacements of the linear and nonlinear solutions can also be noted.

For proportionally damped vibration ($\mathbf{C} = \alpha\mathbf{M}$), where damping ratio $\alpha = 0.1$, $P(t) = F \cos \omega t \, N$ acting at the top point, $\omega = 1.1 \, \omega_L$, $F = 1200$ kN in which the linear fundamental frequency of symmetry mode $\omega_L = 275.844$ rad/s. The time-centered Euler scheme with variable time step is used. The response curves are shown in Fig. 12(a–c). For a linear response, solutions obtained using the whole frame are in agreement with those obtained using one half of the frame. Figure 12(a–c) shows that the difference between the linear and nonlinear responses and the difference between solutions obtained using one-half of the frame and using the whole frame still exist.

CONCLUSIONS

Symplectic methods are successful in integrating the Hamiltonian equations of skeletal structures consisting of beam elements developed by Leung and Mao (1995). The equations of motion are integrated element by element which avoids the formation of a global stiffness matrices so that complicated framed structures with many elements can be handled in core. The present method is efficient for dynamic and geometric analyses. Dynamic symmetry breaking is demonstrated. The response after symmetry breaking is an order higher that cannot be overlooked in a
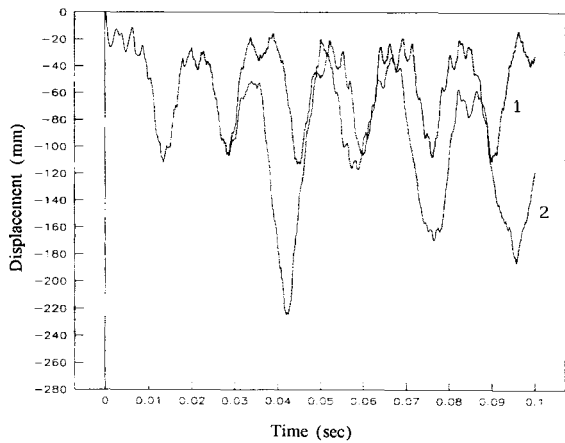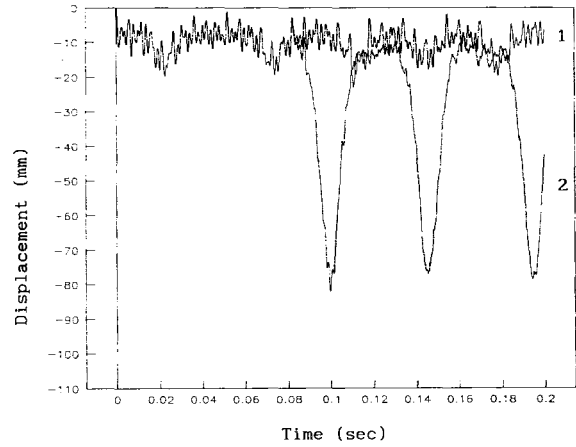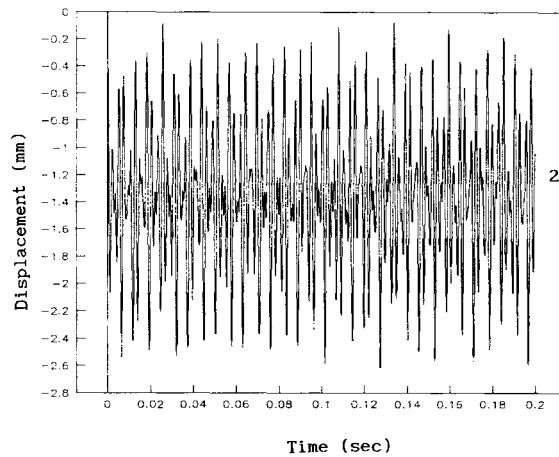
(a) Using the first order scheme, F_c = 1200 KN
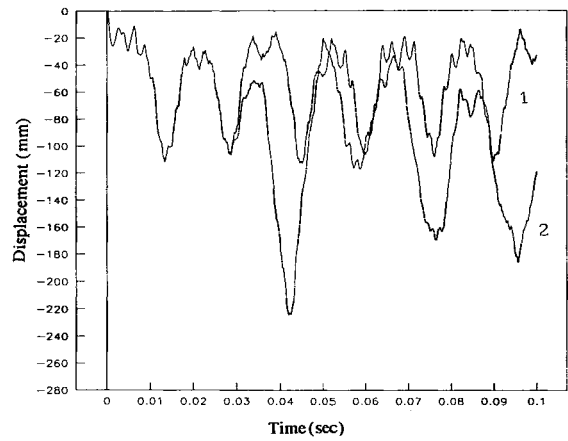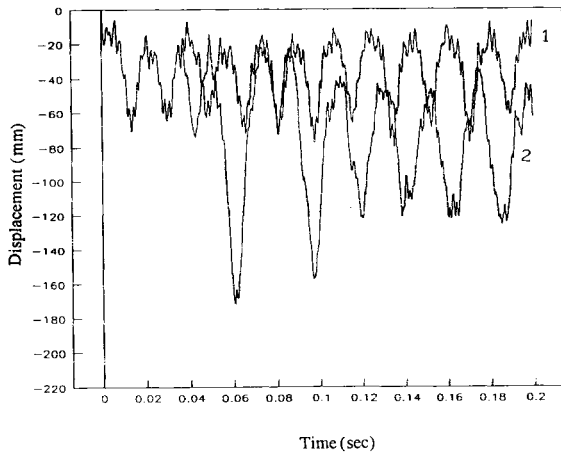
(b) Using time-centered Euler scheme, F_c = 1200 KN

(c) Using time-centered Euler scheme, F_c = 1000 KN

(d) Using time-centered Euler scheme, F_c = 600 KN

(e) Linear solution in time-centered Euler scheme, F_c = 120 KN

FIGURE 10   Vertical Displacement at the top point of plane frame without damping for different loads F_c, curve 1 obtained using one half of frame, curve 2 obtained using whole frame. (a) Using the first order scheme, F_c = 1200 KN; (b) Using time-centered Euler scheme, F_c = 1200 KN; (c) Using time-centered Euler scheme, F_c = 1000 KN; (d) Using time-centered Euler scheme, F_c = 600 KN; (e) Linear solution in time-centered Euler scheme, F_c = 120 KN.

(a) Horizontal displacement

(b) Vertical displacement
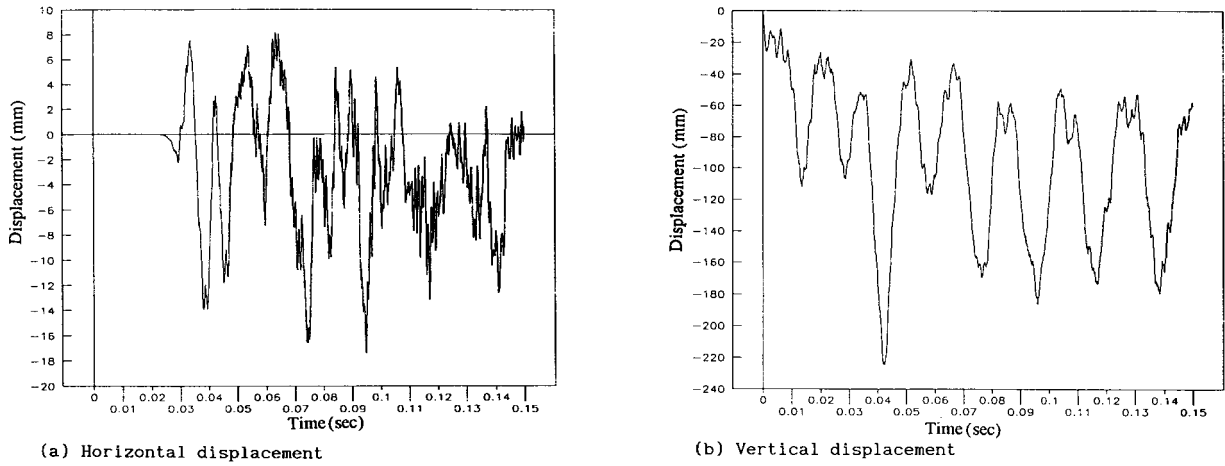
FIGURE 11 Displacement at top point of a plane frame for $F_c = 1200$ KN, using whole frame, (a) horizontal displacement; (b) vertical displacement.

(a) linear solution using whole frame

(b) Nonlinear solution using one half of frame
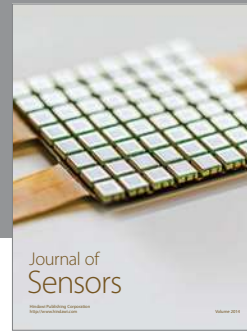
(c) Nonlinear solution using whole frame
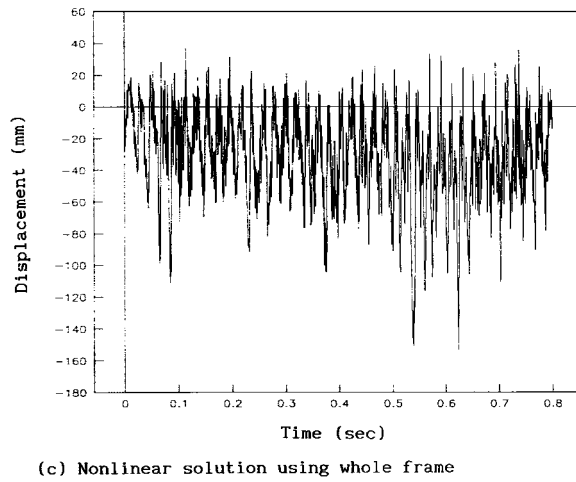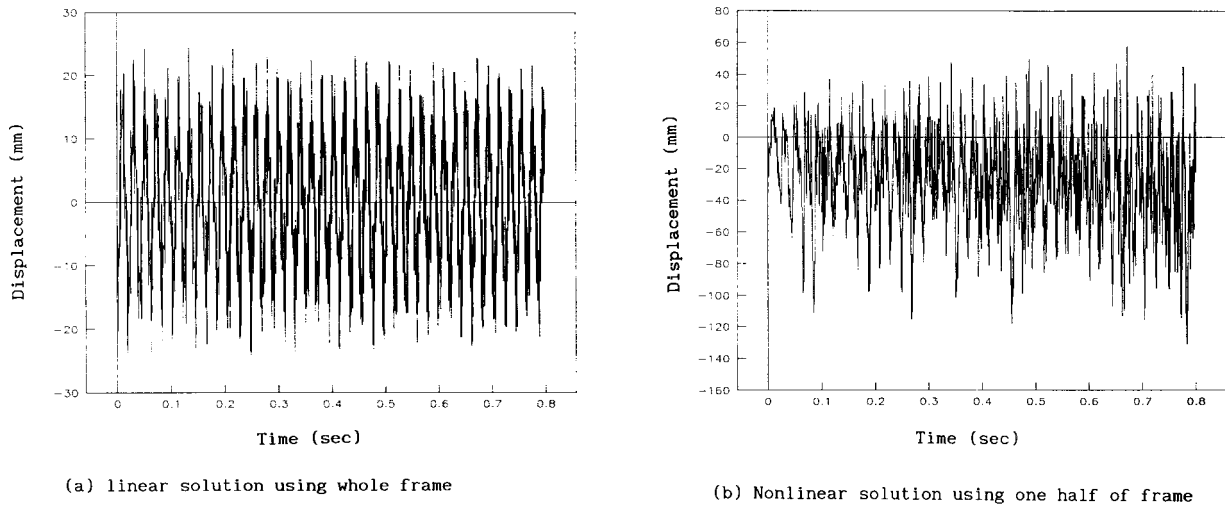
FIGURE 12 Vertical Displacement at the top point of plane frame with damping; (a) linear solution using whole frame; (b) nonlinear solution using one half of frame; (c) nonlinear solution using whole frame.

structural design. It is advisable to use the whole structure rather than its symmetric portion when nonlinear dynamic response is of interest.

REFERENCES

Abraham, R., and Marsden, J. E., 1978, Foundations of Mechanics, 2nd ed., Bejamin/Cummings, Reading, MA.

Arnold, V. I., 1978, Mathematical Method of Classical Mechanics, Springer–Verlag, New York.

Bathe, K. J., Ramm, E., and Wilson, E. L., 1975, "Finite Element Formulations for Large Deformation Dynamic Analysis," International Journal of Numerical Methods in Engineering, Vol. 9, pp. 353–386.

Chajes, A., and Churchill, J. E., 1987, "Nonlinear Frame Analysis by Finite Element Methods," Journal of Structural Engineering, ASCE, Vol. 113, pp. 1221–1235.

Crisfield, M. A., 1991, Nonlinear Finite Element Analysis of Solids and Structures, Wiley, New York.

Crisfield, M. A., and Shi, J., 1994, "A Co-Rotational Element/Time-Integration Strategy for Non-Linear Dynamics," International Journal of Numerical Methods in Engineering, Vol. 37, pp. 1897–1913.

Feng, K., and Qin, M. Z., 1991, "Hamiltonian Algorithms for Hamiltonian Systems and a Comparative Numerical Study," Computer Physics Communications, Vol. 65, pp. 173–187.

Feng, K., Wu, H. M., Qin, M. Z., and Wang, D. L., 1989, "Construction of Canonical Difference Schemes for Hamiltonian Formalism Via Generating Functions," Journal of Computational Mathematics, Vol. 7, pp. 71–96.

Goldstein, H., 1980, Classical Mechanics, Addison–Wesley, Reading, MA.

Leung, A. Y. T., and Mao, S. G., 1995, "Symplectic

Integration of an Accurate Beam Finite Element in Nonlinear Vibration," Computers & Structures, Vol. 54, pp. 1135–1147.

McNamara, J. E., 1974, "Solutions Schemes for Problems of Nonlinear Structural Dynamics," Journal of Pressure Vessel Technology, ASME, vol. 96, pp. 96–102.

Meek, J. L., and Tan, H. S., 1984, "Geometrically Nonlinear Analysis of Space Frames by an Incremental Iterative Technique," Computer Methods in Applied Mechanics and Engineering, Vol. 47, pp. 261–282.

Mondkar, D. P., and Powell, G. H., 1977, "Finite Element Analysis of Nonlinear Static and Dynamic Response," International Journal of Numerical Methods in Engineering, Vol. 11, pp. 499–520.

Qin, M. Z., Wang, D. L., and Zhang, M. Q., 1991, "Explicit Symplectic Difference Schemes for Separable Hamiltonian Systems," Journal of Computational Mathematics, Vol. 9, pp. 211–221.

Robert, I. M., and Pau, A., 1992, "The Accuracy of Symplectic Integrators," Nonlinearity, Vol. 5, pp. 541–556.

Ruth, R. D., 1983, "A Canonical Integration Technique," IEEE Transactions on Nuclear Science, Vol. NS-30, pp. 2669–2671.

Simo, J. C., Tarnow, N., and Wong, K. K., 1992, "Exact Energy-Momentum Conserving Algorithms and Symplectic Schemes for Nonlinear Dynamics," Computer Methods in Applied Mechanics and Engineering, Vol. 100, pp. 63–116.

Wood, R. D., and Zienkiewicz, O. C., 1977, "Geometrically Nonlinear Finite Element Analysis of Beams, Frames, Arches and Axisymmetric Shells," Computers & Structures, Vol. 7, pp. 725–735.

Wu, Y. 1988, "The Generating Functions for the Solution of ODEs and Its Discrete Methods," Computational Mathematics and Applications, Vol. 15, pp. 1041–1050.

Yang, T. Y., and Saigal, S., 1984, "A Simple Element for Static and Dynamic Response of Beams with Material and Geometric Nonlinearities," International Journal of Numerical Methods in Engineering, Vol. 20, pp. 851–867.